SCIENTIFIC OASIS

Journal of Intelligent Decision Making and Granular Computing

Journal homepage: www.jidmag.org
ISSN: 3042-3759

Application of New Divergence Measure in Complex Fermatean Fuzzy Sets for Post-Flood Assessment

Yuhan Li[1], Sijia Zhu[2], Juan Liao[3,4], Sukumar Letchmunan[3,*], Jiahao Shi[5], Zhe Liu[3,6,*]

[1] Cw Chu College, Jiangsu Normal University, Xuzhou 221116, China
[2] Department of Applied Mathematics and Statistics, Johns Hopkins University, Baltimore 21218, USA
[3] School of Computer Sciences, Universiti Sains Malaysia, Penang 11800, Malaysia
[4] School of Big Data Engineering, Kaili University, Kaili 556000, China
[5] College of Computer Science and Technology, Harbin Engineering University, Harbin 150001, China
[6] College of Mathematics and Computer, Xinyu University, Xinyu 338004, China

ARTICLE INFO

Article history:
Received 13 April 2025
Received in revised form21 May 2025
Accepted 1 July 2025
Available online 12 July 2025

Keywords:
Complex Fermatean fuzzy sets; Divergence measures; Decision-making; Post-flood assessment

ABSTRACT

Complex Fermatean fuzzy sets (CFFSs) combine complex fuzzy sets and Fermatean fuzzy sets, with membership, non-membership, and neutral degrees represented as complex numbers, thus enabling a more flexible and comprehensive representation of uncertainty. Nevertheless, a key unresolved challenge is how to measure the differences of CFFSs in decision-making processes appropriately. This paper introduces a new divergence measure based on CFFSs, aiming to overcome the limitations of existing measures. The proposed measure has been thoroughly validated to meet the required axioms, with its reliability and effectiveness confirmed through numerical comparisons. Additionally, we apply the proposed divergence measures to a post-flood assessment application, demonstrating their high confidence and consistency.

1. Introduction

In decision-making, uncertainty and vagueness are pervasive and extend into virtually all areas of daily life [1, 2]. Addressing such uncertainty has become a key challenge in decision-making processes [3]. In recent years, several theories such as fuzzy sets [4, 5], complex fuzzy sets [6, 7], and evidence theory [8] have been developed to address such issues. Fuzzy set theory, introduced by Zadeh [9], marked a key development in this field. Fuzzy sets (FSs), based on membership degrees, provide a way to handle uncertainty beyond traditional set theory. Following this, Atanassov [10] introduced intuitionistic fuzzy sets (IFSs) with membership and non-membership degrees, widely used in decision-

*Corresponding authors.
E-mail address: sukumar@usm.my; liuzhe921@gmail.com

https://doi.org/10.31181/jidmgc1120258

making [11, 12]. In IFSs, the sum of membership and non-membership degrees can not exceed one, limiting their use in some instances. Yger [13] further extended IFSs to Pythagorean fuzzy sets (PFSs) and have been employed to address decision-making problems [14–16]. Nevertheless, in PFSs, the squares of the membership and non-membership degrees add up to no more than one. To address this issue, Senapati and Yager [17] proposed Fermatean fuzzy sets (FFSs), in which the sum of the cubes of the membership and non-membership degrees does not exceed one. Likewise, FFSs have garnered considerable interest and found application in decision-making contexts [18, 19].

However, the fuzzy sets discussed above are limited to the real number domain and cannot be extended to complex-valued settings. To bridge this gap, Ramot *et al.* [20] introduced complex fuzzy sets (CFSs), extending membership functions into the complex domain to provide a new perspective on uncertainty modeling. As an extension of CFSs, complex intuitionistic fuzzy sets (CIFSs) were introduced by Alkouri *et al.* [21] to express both membership and non-membership degrees using complex numbers. Several studies concerning CIFSs have emerged in recent years [22, 23]. Yet, like IFSs, the sum of the membership and non-membership degrees in CIFSs must not exceed one. As a result, Ullah *et al.* [24] proposed complex Pythagorean fuzzy sets (CPFSs) and have been widely acknowledged in subsequent research [25–27]. For instance, Labassi *et al.* [25] developed a Cartesian-based CPFS framework and tailored aggregation operators to enhance logical operations and decision-making. Khan [26] proposed CPFS-based decision-making tools for green supply chain problems. Recently, Akram *et al.* [28] introduced complex Fermatean fuzzy sets (CFFSs) to capture uncertain complex-valued information more effectively. Up to now, CFFSs have attracted some attention in the research community [6, 29, 30].

Distance/divergence measures are key topics in fuzzy sets and have gained much attention from researchers [31–33]. So far, various distance or divergence measures have been proposed for IFSs, PFSs, and FFSs. For example, Gohain *et al.* [34] developed a symmetric distance measure for IFSs and proved effective in applications such as decision-making, pattern recognition, and clustering. Subsequently, Ganie *et al.* [35] introduced a novel distance measure under the FFS framework, incorporating all three membership functions, and demonstrated its effectiveness in pattern classification. Wu *et al.* [33] proposed a new Jensen–Shannon divergence measure for IFSs and demonstrated its effectiveness in multi-attribute decision-making through a credit evaluation case study. In recent years, several works have focused on developing distance or similarity measures for CIFSs and CPFSs. For instance, Rani and Garg [36] developed new distance measures for CIFSs and applied them to decision-making problems in pattern recognition and medical diagnosis. Ullah *et al.* [37] presented CPFSs, established their fundamental properties and distance measures and validated their effectiveness through a material recognition problem. There has been a growing research interest in distance/divergence measures for CFFSs in recent studies. Liu *et al.* [6] proposed new distance measures for CFFSs based on classical metrics, and applied them to decision-making and clustering tasks to demonstrate their effectiveness.

Motivation: On the one hand, many traditional fuzzy sets have some drawbacks in real-world applications. For example, although CIFSs include complex-valued membership ($\mathscr{P}$) and non-membership ($\mathscr{Q}$) degrees, they are limited by the condition: $\mathscr{P}^2 + \mathscr{Q}^2 \leqslant 1$. In comparison, CFFSs use a more flexible rule: $\mathscr{P}^3 + \mathscr{Q}^3 \leqslant 1$. This condition performs better and can better capture the complex interaction between membership and non-membership. On the other hand, there are few studies on distance or similarity measures for CFFSs. Therefore, it is necessary to propose new measures to fill this gap and extend their use in applications.

Methods: This paper presents a new divergence measure for CFFSs, whose main properties are then analyzed and formally proved. Finally, we apply the divergence measure to a post-flood assessment application based on CFFSs.

Contributions: The main contributions of this paper are summarized as follows:

- We propose a novel divergence measure for CFFSs.

- We analyze and prove the main theorems related to the proposed divergence measure.
- We demonstrate the advantages of the proposed measure over existing ones through numerical comparisons.
- We apply the proposed divergence measure to a post-flood assessment application to demonstrate its higher confidence and reliability compared to existing measures.

The structure of this paper is organized as follows: Section 2 reviews the basic concepts and presents the existing distance measures. Section 3 introduces a new divergence measure for CFFSs and proves that it satisfies the related properties. Section 4 provides numerical comparisons between the existing distance measures and the proposed divergence measure. Section 5 applies the proposed divergence measure to a post-flood assessment application. Section 6 makes a conclusion.

2. Preliminaries

This section outlines the key concepts of fuzzy sets and reviews the existing distance measures for CFFSs.

2.1 Key Concepts of Fuzzy Sets

Definition 1 *[10] Consider $\mathit{\Gamma} = \{\varsigma_1, \varsigma_2, ..., \varsigma_n\}$ be a universe of discourse (UOD). An intuitionistic fuzzy set (IFS) in $\mathit{\Gamma}$ can be described as follows:*

$$\mathcal{I} = \{\langle \varsigma_t, \mathscr{P}_{\mathcal{I}}(\varsigma_t), \mathscr{Q}_{\mathcal{I}}(\varsigma_t)\rangle | \varsigma_t \in \mathit{\Gamma}\} \tag{1}$$

where $\mathscr{P}_{\mathcal{I}}, \mathscr{Q}_{\mathcal{I}} : \mathit{\Gamma} \to [0,1]$ denote the membership and non-membership degrees. Given any $\varsigma_t \in \mathit{\Gamma}$, it follows that

$$0 \leqslant \mathscr{P}_{\mathcal{I}}(\varsigma_t) + \mathscr{Q}_{\mathcal{I}}(\varsigma_t) \leqslant 1 \quad \text{and} \quad \mathscr{R}_{\mathcal{U}}(\varsigma_t) = 1 - \mathscr{P}_{\mathcal{I}}(\varsigma_t) - \mathscr{Q}_{\mathcal{I}}(\varsigma_t)$$

where $\mathscr{R}_{\mathcal{U}} : \mathit{\Gamma} \to [0,1]$ represents the degree of neutral.

Definition 2 *[21] A complex intuitionistic fuzzy set (CIFS) in $\mathit{\Gamma}$ is represented as:*

$$\mathcal{U} = \{\langle \varsigma_t, \mathscr{P}_{\mathcal{U}}(\varsigma_t), \mathscr{Q}_{\mathcal{U}}(\varsigma_t)\rangle | \varsigma_t \in \mathit{\Gamma}\} \tag{2}$$

where $\mathscr{P}_{\mathcal{U}}, \mathscr{Q}_{\mathcal{U}} : \mathit{\Gamma} \to \{z : z \in C, |z| \leqslant 1\}$ denote the degrees of complex-valued membership and non-membership, respectively, and are given by:

$$\mathscr{P}_{\mathcal{U}}(\varsigma_t) = \wp_{\mathcal{U}}(\varsigma_t)\, e^{2\pi i W_{\wp_{\mathcal{U}}(\varsigma_t)}}, \;\; \mathscr{Q}_{\mathcal{U}}(\varsigma_t) = \gamma_{\mathcal{U}}(\varsigma_t)\, e^{2\pi i W_{\gamma_{\mathcal{U}}(\varsigma_t)}}$$

where $\wp_{\mathcal{U}}(\varsigma_t), \gamma_{\mathcal{U}}(\varsigma_t) \in [0,1]$ and $0 \leqslant \wp_{\mathcal{U}}(\varsigma_t) + \gamma_{\mathcal{U}}(\varsigma_t) \leqslant 1$. Similarly, $W_{\wp_{\mathcal{U}}(\varsigma_t)}, W_{\gamma_{\mathcal{U}}(\varsigma_t)} \in [0,1]$ and $0 \leqslant W_{\wp_{\mathcal{U}}(\varsigma_t)} + W_{\gamma_{\mathcal{U}}(\varsigma_t)} \leqslant 1$. Moreover, the neutral degree is referred to as:

$$\mathscr{R}_{\mathcal{U}}(\varsigma_t) = 1 - \mathscr{P}_{\mathcal{U}}(\varsigma_t) - \mathscr{Q}_{\mathcal{U}}(\varsigma_t) = \eta_{\mathcal{U}}(\varsigma_t)\, e^{2\pi i W_{\eta_{\mathcal{U}}(\varsigma_t)}}$$

where $\eta_{\mathcal{U}}(\varsigma_t) = 1 - \wp_{\mathcal{U}}(\varsigma_t) - \gamma_{\mathcal{U}}(\varsigma_t)$ and $W_{\eta_{\mathcal{U}}(\varsigma_t)} = 1 - W_{\wp_{\mathcal{U}}(\varsigma_t)} - W_{\gamma_{\mathcal{U}}(\varsigma_t)}$.

Definition 3 *[13] A Pythagorean fuzzy set (PFS) in Γ is defined as follows:*

$$\mathcal{I}=\{\langle \varsigma_t, \mathscr{P}_{\mathcal{I}}(\varsigma_t), \mathscr{Q}_{\mathcal{I}}(\varsigma_t)\rangle \mid \varsigma_t \in \Gamma\} \tag{3}$$

where $\mathscr{P}_{\mathcal{I}}, \mathscr{Q}_{\mathcal{I}} : \Gamma \rightarrow [0,1]$ express the membership and non-membership degrees. Given any $\varsigma_t \in \Gamma$, it follows that

$$0 \leqslant \mathscr{P}_{\mathcal{I}}^2(\varsigma_t)+\mathscr{Q}_{\mathcal{I}}^2(\varsigma_t) \leqslant 1 \quad \text{and} \quad \mathscr{R}_{\mathcal{U}}(\varsigma_t)=\sqrt{1-\mathscr{P}_{\mathcal{I}}^2(\varsigma_t)-\mathscr{Q}_{\mathcal{I}}^2(\varsigma_t)}$$

where $\mathscr{R}_{\mathcal{U}} : \Gamma \rightarrow [0,1]$ represents the degree of neutral.

Definition 4 *[24] A complex Pythagorean fuzzy set (CPFS) in Γ is stated as:*

$$\mathcal{U}=\{\langle \varsigma_t, \mathscr{P}_{\mathcal{U}}(\varsigma_t), \mathscr{Q}_{\mathcal{U}}(\varsigma_t)\rangle \mid \varsigma_t \in \Gamma\} \tag{4}$$

where $\mathscr{P}_{\mathcal{U}}, \mathscr{Q}_{\mathcal{U}} : \Gamma \rightarrow \{z : z \in C, |z| \leqslant 1\}$ denote the degrees of complex-valued membership and non-membership, respectively, and are given by:

$$\mathscr{P}_{\mathcal{U}}(\varsigma_t)=\wp_{\mathcal{U}}(\varsigma_t)\, e^{2\pi i W_{\wp_{\mathcal{U}}(\varsigma_t)}},\ \mathscr{Q}_{\mathcal{U}}(\varsigma_t)=\gamma_{\mathcal{U}}(\varsigma_t)\, e^{2\pi i W_{\gamma_{\mathcal{U}}(\varsigma_t)}}$$

where $\wp_{\mathcal{U}}(\varsigma_t), \gamma_{\mathcal{U}}(\varsigma_t) \in [0,1]$ and $0 \leqslant \wp_{\mathcal{U}}^2(\varsigma_t)+\gamma_{\mathcal{U}}^2(\varsigma_t) \leqslant 1$. Similarly, $W_{\wp_{\mathcal{U}}(\varsigma_t)}, W_{\gamma_{\mathcal{U}}(\varsigma_t)} \in [0,1]$ and $0 \leqslant W_{\wp_{\mathcal{U}}(\varsigma_t)}^2+W_{\gamma_{\mathcal{U}}(\varsigma_t)}^2 \leqslant 1$. Moreover, the neutral degree is referred to as:

$$\mathscr{R}_{\mathcal{U}}(\varsigma_t)=\sqrt{1-\mathscr{P}_{\mathcal{U}}^2(\varsigma_t)-\mathscr{Q}_{\mathcal{U}}^2(\varsigma_t)}=\eta_{\mathcal{U}}(\varsigma_t)\, e^{2\pi i W_{\eta_{\mathcal{U}}(\varsigma_t)}}$$

where $\eta_{\mathcal{U}}(\varsigma_t)=\sqrt{1-\wp_{\mathcal{U}}^2(\varsigma_t)-\gamma_{\mathcal{U}}^2(\varsigma_t)}$ and $W_{\eta_{\mathcal{U}}(\varsigma_t)}=\sqrt{1-W_{\wp_{\mathcal{U}}(\varsigma_t)}^2-W_{\gamma_{\mathcal{U}}(\varsigma_t)}^2}$.

Definition 5 *[17] A Fermatean fuzzy set (FFS) in Γ is represented as follows:*

$$\mathcal{I}=\{\langle \varsigma_t, \mathscr{P}_{\mathcal{I}}(\varsigma_t), \mathscr{Q}_{\mathcal{I}}(\varsigma_t)\rangle \mid \varsigma_t \in \Gamma\} \tag{5}$$

where $\mathscr{P}_{\mathcal{I}}, \mathscr{Q}_{\mathcal{I}} : \Gamma \rightarrow [0,1]$ express the membership and non-membership degrees. Given any $\varsigma_t \in \Gamma$, it follows that

$$0 \leqslant \mathscr{P}_{\mathcal{I}}^3(\varsigma_t)+\mathscr{Q}_{\mathcal{I}}^3(\varsigma_t) \leqslant 1 \quad \text{and} \quad \mathscr{R}_{\mathcal{U}}(\varsigma_t)=\sqrt[3]{1-\mathscr{P}_{\mathcal{I}}^3(\varsigma_t)-\mathscr{Q}_{\mathcal{I}}^3(\varsigma_t)}$$

where $\mathscr{R}_{\mathcal{U}} : \Gamma \rightarrow [0,1]$ denotes the degree of neutral.

Definition 6 *[28] A complex Fermatean fuzzy set (CFFS) in Γ is expressed as:*

$$\mathcal{U}=\{\langle \varsigma_t, \mathscr{P}_{\mathcal{U}}(\varsigma_t), \mathscr{Q}_{\mathcal{U}}(\varsigma_t)\rangle \mid \varsigma_t \in \Gamma\} \tag{6}$$

where $\mathscr{P}_{\mathcal{U}}, \mathscr{Q}_{\mathcal{U}} : \Gamma \rightarrow \{z : z \in C, |z| \leqslant 1\}$ denote the degrees of complex-valued membership and non-membership, respectively, and are given by:

$$\mathscr{P}_{\mathcal{U}}(\varsigma_t)=\wp_{\mathcal{U}}(\varsigma_t)\, e^{2\pi i W_{\wp_{\mathcal{U}}(\varsigma_t)}},\ \mathscr{Q}_{\mathcal{U}}(\varsigma_t)=\gamma_{\mathcal{U}}(\varsigma_t)\, e^{2\pi i W_{\gamma_{\mathcal{U}}(\varsigma_t)}}$$

where $\wp_{\mathcal{U}}(\varsigma_t), \gamma_{\mathcal{U}}(\varsigma_t) \in [0,1]$ and $0 \leqslant \wp_{\mathcal{U}}^3(\varsigma_t)+\gamma_{\mathcal{U}}^3(\varsigma_t) \leqslant 1$. Similarly, $W_{\wp_{\mathcal{U}}(\varsigma_t)}, W_{\gamma_{\mathcal{U}}(\varsigma_t)} \in [0,1]$ and $0 \leqslant W_{\wp_{\mathcal{U}}(\varsigma_t)}^3+W_{\gamma_{\mathcal{U}}(\varsigma_t)}^3 \leqslant 1$. Moreover, the neutral degree is referred to as:

$$\mathscr{R}_{\mathcal{U}}(\varsigma_t)=\sqrt[3]{1-\mathscr{P}_{\mathcal{U}}^3(\varsigma_t)-\mathscr{Q}_{\mathcal{U}}^3(\varsigma_t)}=\eta_{\mathcal{U}}(\varsigma_t)\, e^{2\pi i W_{\eta_{\mathcal{U}}(\varsigma_t)}}$$

where $\eta_{\mathcal{U}}(\varsigma_t)=\sqrt[3]{1-\wp_{\mathcal{U}}^3(\varsigma_t)-\gamma_{\mathcal{U}}^3(\varsigma_t)}$ and $W_{\eta_{\mathcal{U}}(\varsigma_t)}=\sqrt[3]{1-W_{\wp_{\mathcal{U}}(\varsigma_t)}^3-W_{\gamma_{\mathcal{U}}(\varsigma_t)}^3}$.

2.2 Existing Distance Measures for CFFSs

This subsection introduces the existing distance measures for CFFSs. The shortcomings of these measures and their comparisons will be discussed in Section 4. The existing distance measures for CFFSs proposed by Liu *et al.* [6] are presented below:
The 2D Hamming distance measure for CFFSs:

$$\mathbb{D}^1_{Ham}(\mathcal{U}\|\mathcal{V}) = \frac{1}{4n}\sum_{t=1}^{n}\left[\begin{array}{c} \left|\wp^3_{\mathcal{U}}(\varsigma_t) - \wp^3_{\mathcal{V}}(\varsigma_t)\right| + \left|\gamma^3_{\mathcal{U}}(\varsigma_t) - \gamma^3_{\mathcal{V}}(\varsigma_t)\right| + \\ \left|W^3_{\wp_{\mathcal{U}}}(\varsigma_t) - W^3_{\wp_{\mathcal{V}}}(\varsigma_t)\right| + \left|W^3_{\gamma_{\mathcal{U}}}(\varsigma_t) - W^3_{\gamma_{\mathcal{V}}}(\varsigma_t)\right| \end{array}\right] \tag{7}$$

The 3D Hamming distance measure for CFFSs:

$$\mathbb{D}^2_{Ham}(\mathcal{U}\|\mathcal{V}) = \frac{1}{4n}\sum_{t=1}^{n}\left[\begin{array}{c} \left|\wp^3_{\mathcal{U}}(\varsigma_t) - \wp^3_{\mathcal{V}}(\varsigma_t)\right| + \left|\gamma^3_{\mathcal{U}}(\varsigma_t) - \gamma^3_{\mathcal{V}}(\varsigma_t)\right| \\ + \left|\eta^3_{\mathcal{U}}(\varsigma_t) - \eta^3_{\mathcal{V}}(\varsigma_t)\right| + \left|W^3_{\wp_{\mathcal{U}}}(\varsigma_t) - W^3_{\wp_{\mathcal{V}}}(\varsigma_t)\right| \\ + \left|W^3_{\gamma_{\mathcal{U}}}(\varsigma_t) - W^3_{\gamma_{\mathcal{V}}}(\varsigma_t)\right| + \left|W^3_{\eta_{\mathcal{U}}}(\varsigma_t) - W^3_{\eta_{\mathcal{V}}}(\varsigma_t)\right| \end{array}\right] \tag{8}$$

The 2D Euclidean distance measure for CFFSs:

$$\mathbb{D}^1_{Eu}(\mathcal{U}\|\mathcal{V}) = \sqrt{\frac{1}{4n}\sum_{t=1}^{n}\left[\begin{array}{c} \left(\wp^3_{\mathcal{U}}(\varsigma_t) - \wp^3_{\mathcal{V}}(\varsigma_t)\right)^2 + \left(\gamma^3_{\mathcal{U}}(\varsigma_t) - \gamma^3_{\mathcal{V}}(\varsigma_t)\right)^2 \\ + \left(W^3_{\wp_{\mathcal{U}}}(\varsigma_t) - W^3_{\wp_{\mathcal{V}}}(\varsigma_t)\right)^2 + \left(W^3_{\gamma_{\mathcal{U}}}(\varsigma_t) - W^3_{\gamma_{\mathcal{V}}}(\varsigma_t)\right)^2 \end{array}\right]} \tag{9}$$

The 3D Euclidean distance measure for CFFSs:

$$\mathbb{D}^2_{Eu}(\mathcal{U}\|\mathcal{V}) = \sqrt{\frac{1}{4n}\sum_{t=1}^{n}\left[\begin{array}{c} \left(\wp^3_{\mathcal{U}}(\varsigma_t) - \wp^3_{\mathcal{V}}(\varsigma_t)\right)^2 + \left(\gamma^3_{\mathcal{U}}(\varsigma_t) - \gamma^3_{\mathcal{V}}(\varsigma_t)\right)^2 \\ + \left(\eta^3_{\mathcal{U}}(\varsigma_t) - \eta^3_{\mathcal{V}}(\varsigma_t)\right)^2 + \left(W^3_{\wp_{\mathcal{U}}}(\varsigma_t) - W^3_{\wp_{\mathcal{V}}}(\varsigma_t)\right)^2 \\ + \left(W^3_{\gamma_{\mathcal{U}}}(\varsigma_t) - W^3_{\gamma_{\mathcal{V}}}(\varsigma_t)\right)^2 + \left(W^3_{\eta_{\mathcal{U}}}(\varsigma_t) - W^3_{\eta_{\mathcal{V}}}(\varsigma_t)\right)^2 \end{array}\right]} \tag{10}$$

The 2D Hausdorff distance measure for CFFSs:

$$\mathbb{D}^1_{Hau}(\mathcal{U}\|\mathcal{V}) = \frac{1}{2n}\sum_{t=1}^{n}\left(\begin{array}{c} \max\left\{\left|\wp^3_{\mathcal{U}}(\varsigma_t) - \wp^3_{\mathcal{V}}(\varsigma_t)\right|, \left|\gamma^3_{\mathcal{U}}(\varsigma_t) - \gamma^3_{\mathcal{V}}(\varsigma_t)\right|\right\} \\ + \max\left\{\left|W^3_{\wp_{\mathcal{U}}}(\varsigma_t) - W^3_{\wp_{\mathcal{V}}}(\varsigma_t)\right|, \left|W^3_{\gamma_{\mathcal{U}}}(\varsigma_t) - W^3_{\gamma_{\mathcal{V}}}(\varsigma_t)\right|\right\} \end{array}\right) \tag{11}$$

The 3D Hausdorff distance measure for CFFSs:

$$\mathbb{D}^2_{Hau}(\mathcal{U}\|\mathcal{V}) = \frac{1}{2n}\sum_{t=1}^{n}\left(\begin{array}{c} \max\left\{\begin{array}{c} \left|\wp^3_{\mathcal{U}}(\varsigma_t) - \wp^3_{\mathcal{V}}(\varsigma_t)\right|, \left|\gamma^3_{\mathcal{U}}(\varsigma_t) - \gamma^3_{\mathcal{V}}(\varsigma_t)\right|, \\ \left|\eta^3_{\mathcal{U}}(\varsigma_t) - \eta^3_{\mathcal{V}}(\varsigma_t)\right| \end{array}\right\} \\ + \max\left\{\begin{array}{c} \left|W^3_{\wp_{\mathcal{U}}}(\varsigma_t) - W^3_{\wp_{\mathcal{V}}}(\varsigma_t)\right|, \left|W^3_{\gamma_{\mathcal{U}}}(\varsigma_t) - W^3_{\gamma_{\mathcal{V}}}(\varsigma_t)\right|, \\ \left|W^3_{\eta_{\mathcal{U}}}(\varsigma_t) - W^3_{\eta_{\mathcal{V}}}(\varsigma_t)\right| \end{array}\right\} \end{array}\right) \tag{12}$$

The Hellinger distance measure for CFFSs:

$$\mathbb{D}_{He}(\mathcal{U}\|\mathcal{V}) = \sqrt{\frac{1}{4n}\sum_{t=1}^{n}\left[\begin{array}{c} \left(\sqrt{\wp^3_{\mathcal{U}}(\varsigma_t)} - \sqrt{\wp^3_{\mathcal{V}}(\varsigma_t)}\right)^2 + \left(\sqrt{\gamma^3_{\mathcal{U}}(\varsigma_t)} - \sqrt{\gamma^3_{\mathcal{V}}(\varsigma_t)}\right)^2 \\ + \left(\sqrt{W^3_{\wp_{\mathcal{U}}}(\varsigma_t)} - \sqrt{W^3_{\wp_{\mathcal{V}}}(\varsigma_t)}\right)^2 + \left(\sqrt{W^3_{\gamma_{\mathcal{U}}}(\varsigma_t)} - \sqrt{W^3_{\gamma_{\mathcal{V}}}(\varsigma_t)}\right)^2 \end{array}\right]} \tag{13}$$

3. New Divergence Measure for CFFSs

This section introduces a new divergence measure for CFFSs, explaining it for CFFSs $\mathcal{U}$ and $\mathcal{V}$. Additionally, we prove the properties of the proposed divergence measure.

Definition 7 *The new divergence measure between CFFSs $\mathcal{U}$ and $\mathcal{V}$ is defined as follows:*

$$\mathbb{D}_T\left(\mathcal{U}\left\|\mathcal{V}\right.\right)=\frac{1}{4n}\sum_{t=1}^{n}\left[\begin{array}{c}\frac{\left(\wp_{\mathcal{U}}^3(\varsigma_t)-\wp_{\mathcal{V}}^3(\varsigma_t)\right)^2}{\wp_{\mathcal{U}}^3(\varsigma_t)+\wp_{\mathcal{V}}^3(\varsigma_t)}+\frac{\left(\gamma_{\mathcal{U}}^3(\varsigma_t)-\gamma_{\mathcal{V}}^3(\varsigma_t)\right)^2}{\gamma_{\mathcal{U}}^3(\varsigma_t)+\gamma_{\mathcal{V}}^3(\varsigma_t)}\\+\frac{\left(W_{\wp_{\mathcal{U}}}^3(\varsigma_t)-W_{\wp_{\mathcal{V}}}^3(\varsigma_t)\right)^2}{W_{\wp_{\mathcal{U}}}^3(\varsigma_t)+W_{\wp_{\mathcal{V}}}^3(\varsigma_t)}+\frac{\left(W_{\gamma_{\mathcal{U}}}^3(\varsigma_t)-W_{\gamma_{\mathcal{V}}}^3(\varsigma_t)\right)^2}{W_{\gamma_{\mathcal{U}}}^3(\varsigma_t)+W_{\gamma_{\mathcal{V}}}^3(\varsigma_t)}\end{array}\right] \tag{14}$$

Specially, when $\wp_{\mathcal{U}}^3\left(\varsigma_t\right)=\wp_{\mathcal{V}}^3\left(\varsigma_t\right)=0$, we define that $\frac{\left(\wp_{\mathcal{U}}^3(\varsigma_t)-\wp_{\mathcal{V}}^3(\varsigma_t)\right)^2}{\wp_{\mathcal{U}}^3(\varsigma_t)+\wp_{\mathcal{V}}^3(\varsigma_t)}=0$. Others can be defined similarly to the above.

Theorem 1 *Consider three CFFSs, $\mathcal{U}$, $\mathcal{V}$ and $\mathcal{W}$, in UOD Γ. The properties of $\mathbb{D}_T\left(\mathcal{U}\left\|\mathcal{V}\right.\right)$ are described as follows:*

1. $0\leqslant\mathbb{D}_T\left(\mathcal{U}\left\|\mathcal{V}\right.\right)\leqslant 1.$
2. $\mathbb{D}_T\left(\mathcal{U}\left\|\mathcal{V}\right.\right)=0$, *if and only if* $\mathcal{U}=\mathcal{V}$.
3. $\mathbb{D}_T\left(\mathcal{U}\left\|\mathcal{V}\right.\right)=\mathbb{D}_T\left(\mathcal{V}\left\|\mathcal{U}\right.\right)$.
4. *If* $\mathcal{U}\subseteq\mathcal{V}\subseteq\mathcal{W}$, $\mathbb{D}_T\left(\mathcal{U}\left\|\mathcal{V}\right.\right)\leqslant\mathbb{D}_T\left(\mathcal{U}\left\|\mathcal{W}\right.\right)$ *and* $\mathbb{D}_T\left(\mathcal{V}\left\|\mathcal{W}\right.\right)\leqslant\mathbb{D}_T\left(\mathcal{U}\left\|\mathcal{W}\right.\right)$.

Proof 1 *Suppose that $\mathcal{U}$ and $\mathcal{V}$ are two CFFSs in UOD Γ, we can easily obtain $\mathbb{D}_T\left(\mathcal{U}\left\|\mathcal{V}\right.\right)\geqslant 0$. Then, we have:*

$$\begin{aligned}\mathbb{D}_T\left(\mathcal{U}\left\|\mathcal{V}\right.\right)&=\frac{1}{4n}\sum_{t=1}^{n}\left[\begin{array}{c}\frac{\left(\wp_{\mathcal{U}}^3(\varsigma_t)-\wp_{\mathcal{V}}^3(\varsigma_t)\right)^2}{\wp_{\mathcal{U}}^3(\varsigma_t)+\wp_{\mathcal{V}}^3(\varsigma_t)}+\frac{\left(\gamma_{\mathcal{U}}^3(\varsigma_t)-\gamma_{\mathcal{V}}^3(\varsigma_t)\right)^2}{\gamma_{\mathcal{U}}^3(\varsigma_t)+\gamma_{\mathcal{V}}^3(\varsigma_t)}\\+\frac{\left(W_{\wp_{\mathcal{U}}}^3(\varsigma_t)-W_{\wp_{\mathcal{V}}}^3(\varsigma_t)\right)^2}{W_{\wp_{\mathcal{U}}}^3(\varsigma_t)+W_{\wp_{\mathcal{V}}}^3(\varsigma_t)}+\frac{\left(W_{\gamma_{\mathcal{U}}}^3(\varsigma_t)-W_{\gamma_{\mathcal{V}}}^3(\varsigma_t)\right)^2}{W_{\gamma_{\mathcal{U}}}^3(\varsigma_t)+W_{\gamma_{\mathcal{V}}}^3(\varsigma_t)}\end{array}\right]\\&\leqslant\frac{1}{4n}\sum_{t=1}^{n}\left[\begin{array}{c}\frac{\left(\wp_{\mathcal{U}}^3(\varsigma_t)+\wp_{\mathcal{V}}^3(\varsigma_t)\right)^2}{\wp_{\mathcal{U}}^3(\varsigma_t)+\wp_{\mathcal{V}}^3(\varsigma_t)}+\frac{\left(\gamma_{\mathcal{U}}^3(\varsigma_t)+\gamma_{\mathcal{V}}^3(\varsigma_t)\right)^2}{\gamma_{\mathcal{U}}^3(\varsigma_t)+\gamma_{\mathcal{V}}^3(\varsigma_t)}\\+\frac{\left(W_{\wp_{\mathcal{U}}}^3(\varsigma_t)+W_{\wp_{\mathcal{V}}}^3(\varsigma_t)\right)^2}{W_{\wp_{\mathcal{U}}}^3(\varsigma_t)+W_{\wp_{\mathcal{V}}}^3(\varsigma_t)}+\frac{\left(W_{\gamma_{\mathcal{U}}}^3(\varsigma_t)+W_{\gamma_{\mathcal{V}}}^3(\varsigma_t)\right)^2}{W_{\gamma_{\mathcal{U}}}^3(\varsigma_t)+W_{\gamma_{\mathcal{V}}}^3(\varsigma_t)}\end{array}\right]\\&=\frac{1}{4n}\sum_{t=1}^{n}\left[\begin{array}{c}\wp_{\mathcal{U}}^3\left(\varsigma_t\right)+\wp_{\mathcal{V}}^3\left(\varsigma_t\right)+\gamma_{\mathcal{U}}^3\left(\varsigma_t\right)+\gamma_{\mathcal{V}}^3\left(\varsigma_t\right)\\+W_{\wp_{\mathcal{U}}}^3\left(\varsigma_t\right)+W_{\wp_{\mathcal{V}}}^3\left(\varsigma_t\right)+W_{\gamma_{\mathcal{U}}}^3\left(\varsigma_t\right)+W_{\gamma_{\mathcal{V}}}^3\left(\varsigma_t\right)\end{array}\right]\leqslant 1\end{aligned}$$

Therefore, it can be easily concluded that $0\leqslant\mathbb{D}_T\left(\mathcal{U}\left\|\mathcal{V}\right.\right)\leqslant 1$.

Proof 2 *Given $\mathcal{U}=\mathcal{V}$ in UOD Γ, we have:*

$$\wp_{\mathcal{U}}^3\left(\varsigma_t\right)=\wp_{\mathcal{V}}^3\left(\varsigma_t\right),\gamma_{\mathcal{U}}^3\left(\varsigma_t\right)=\gamma_{\mathcal{V}}^3\left(\varsigma_t\right)\ \textit{and}\ W_{\wp_{\mathcal{U}}}^3\left(\varsigma_t\right)=W_{\wp_{\mathcal{V}}}^3\left(\varsigma_t\right),W_{\gamma_{\mathcal{U}}}^3\left(\varsigma_t\right)=W_{\gamma_{\mathcal{V}}}^3\left(\varsigma_t\right)$$

Namely,

$$\wp_{\mathcal{U}}^3\left(\varsigma_t\right)-\wp_{\mathcal{V}}^3\left(\varsigma_t\right)=0,\gamma_{\mathcal{U}}^3\left(\varsigma_t\right)-\gamma_{\mathcal{V}}^3\left(\varsigma_t\right)=0\ \textit{and}\ W_{\wp_{\mathcal{U}}}^3\left(\varsigma_t\right)-W_{\wp_{\mathcal{V}}}^3\left(\varsigma_t\right)=0,W_{\gamma_{\mathcal{U}}}^3\left(\varsigma_t\right)-W_{\gamma_{\mathcal{V}}}^3\left(\varsigma_t\right)=0$$

Hence, it is evident that

$$\mathbb{D}_T\left(\mathcal{U}\left\|\mathcal{V}\right.\right)=\frac{1}{4n}\sum_{t=1}^{n}\left[\begin{array}{c}\frac{\left(\wp_{\mathcal{U}}^3(\varsigma_t)-\wp_{\mathcal{V}}^3(\varsigma_t)\right)^2}{\wp_{\mathcal{U}}^3(\varsigma_t)+\wp_{\mathcal{V}}^3(\varsigma_t)}+\frac{\left(\gamma_{\mathcal{U}}^3(\varsigma_t)-\gamma_{\mathcal{V}}^3(\varsigma_t)\right)^2}{\gamma_{\mathcal{U}}^3(\varsigma_t)+\gamma_{\mathcal{V}}^3(\varsigma_t)}\\+\frac{\left(W_{\wp_{\mathcal{U}}}^3(\varsigma_t)-W_{\wp_{\mathcal{V}}}^3(\varsigma_t)\right)^2}{W_{\wp_{\mathcal{U}}}^3(\varsigma_t)+W_{\wp_{\mathcal{V}}}^3(\varsigma_t)}+\frac{\left(W_{\gamma_{\mathcal{U}}}^3(\varsigma_t)-W_{\gamma_{\mathcal{V}}}^3(\varsigma_t)\right)^2}{W_{\gamma_{\mathcal{U}}}^3(\varsigma_t)+W_{\gamma_{\mathcal{V}}}^3(\varsigma_t)}\end{array}\right]=0$$

Given any $\varsigma_t \in \Gamma$, if $\mathbb{D}_T(\mathcal{U}\|\mathcal{V})=0$, we can obtain:

$$\mathbb{D}_T(\mathcal{U}\|\mathcal{V})=\frac{1}{4n}\sum_{t=1}^{n}\left[\begin{array}{c}\frac{\left(\wp_{\mathcal{U}}^3(\varsigma_t)-\wp_{\mathcal{V}}^3(\varsigma_t)\right)^2}{\wp_{\mathcal{U}}^3(\varsigma_t)+\wp_{\mathcal{V}}^3(\varsigma_t)}+\frac{\left(\gamma_{\mathcal{U}}^3(\varsigma_t)-\gamma_{\mathcal{V}}^3(\varsigma_t)\right)^2}{\gamma_{\mathcal{U}}^3(\varsigma_t)+\gamma_{\mathcal{V}}^3(\varsigma_t)}\\+\frac{\left(W_{\wp_{\mathcal{U}}}^3(\varsigma_t)-W_{\wp_{\mathcal{V}}}^3(\varsigma_t)\right)^2}{W_{\wp_{\mathcal{U}}}^3(\varsigma_t)+W_{\wp_{\mathcal{V}}}^3(\varsigma_t)}+\frac{\left(W_{\gamma_{\mathcal{U}}}^3(\varsigma_t)-W_{\gamma_{\mathcal{V}}}^3(\varsigma_t)\right)^2}{W_{\gamma_{\mathcal{U}}}^3(\varsigma_t)+W_{\gamma_{\mathcal{V}}}^3(\varsigma_t)}\end{array}\right]=0$$

So, we have:

$$\left(\wp_{\mathcal{U}}^3(\varsigma_t)-\wp_{\mathcal{V}}^3(\varsigma_t)\right)^2=0,\left(\gamma_{\mathcal{U}}^3(\varsigma_t)-\gamma_{\mathcal{V}}^3(\varsigma_t)\right)^2=0;$$
$$\left(W_{\wp_{\mathcal{U}}}^3(\varsigma_t)-W_{\wp_{\mathcal{V}}}^3(\varsigma_t)\right)^2=0,\left(W_{\gamma_{\mathcal{U}}}^3(\varsigma_t)-W_{\gamma_{\mathcal{V}}}^3(\varsigma_t)\right)^2=0.$$

Specifically,

$$\wp_{\mathcal{U}}^3(\varsigma_t)=\wp_{\mathcal{V}}^3(\varsigma_t),\gamma_{\mathcal{U}}^3(\varsigma_t)=\gamma_{\mathcal{V}}^3(\varsigma_t)\text{ and }W_{\wp_{\mathcal{U}}}^3(\varsigma_t)=W_{\wp_{\mathcal{V}}}^3(\varsigma_t),W_{\gamma_{\mathcal{U}}}^3(\varsigma_t)=W_{\gamma_{\mathcal{V}}}^3(\varsigma_t)$$

Hence, it is clear that $\mathbb{D}_T(\mathcal{U}\|\mathcal{V})=0$, if and only if $\mathcal{U}=\mathcal{V}$.

Proof 3 *Suppose two CFFSs $\mathcal{U}$ and $\mathcal{V}$ in UOD Γ, we can get:*

$$\begin{aligned}\mathbb{D}_T(\mathcal{U}\|\mathcal{V})&=\frac{1}{4n}\sum_{t=1}^{n}\left[\begin{array}{c}\frac{\left(\wp_{\mathcal{U}}^3(\varsigma_t)-\wp_{\mathcal{V}}^3(\varsigma_t)\right)^2}{\wp_{\mathcal{U}}^3(\varsigma_t)+\wp_{\mathcal{V}}^3(\varsigma_t)}+\frac{\left(\gamma_{\mathcal{U}}^3(\varsigma_t)-\gamma_{\mathcal{V}}^3(\varsigma_t)\right)^2}{\gamma_{\mathcal{U}}^3(\varsigma_t)+\gamma_{\mathcal{V}}^3(\varsigma_t)}\\+\frac{\left(W_{\wp_{\mathcal{U}}}^3(\varsigma_t)-W_{\wp_{\mathcal{V}}}^3(\varsigma_t)\right)^2}{W_{\wp_{\mathcal{U}}}^3(\varsigma_t)+W_{\wp_{\mathcal{V}}}^3(\varsigma_t)}+\frac{\left(W_{\gamma_{\mathcal{U}}}^3(\varsigma_t)-W_{\gamma_{\mathcal{V}}}^3(\varsigma_t)\right)^2}{W_{\gamma_{\mathcal{U}}}^3(\varsigma_t)+W_{\gamma_{\mathcal{V}}}^3(\varsigma_t)}\end{array}\right]\\&=\frac{1}{4n}\sum_{t=1}^{n}\left[\begin{array}{c}\frac{\left(\wp_{\mathcal{V}}^3(\varsigma_t)-\wp_{\mathcal{U}}^3(\varsigma_t)\right)^2}{\wp_{\mathcal{V}}^3(\varsigma_t)+\wp_{\mathcal{U}}^3(\varsigma_t)}+\frac{\left(\gamma_{\mathcal{V}}^3(\varsigma_t)-\gamma_{\mathcal{U}}^3(\varsigma_t)\right)^2}{\gamma_{\mathcal{V}}^3(\varsigma_t)+\gamma_{\mathcal{U}}^3(\varsigma_t)}\\+\frac{\left(W_{\wp_{\mathcal{V}}}^3(\varsigma_t)-W_{\wp_{\mathcal{U}}}^3(\varsigma_t)\right)^2}{W_{\wp_{\mathcal{V}}}^3(\varsigma_t)+W_{\wp_{\mathcal{U}}}^3(\varsigma_t)}+\frac{\left(W_{\gamma_{\mathcal{V}}}^3(\varsigma_t)-W_{\gamma_{\mathcal{U}}}^3(\varsigma_t)\right)^2}{W_{\gamma_{\mathcal{V}}}^3(\varsigma_t)+W_{\gamma_{\mathcal{U}}}^3(\varsigma_t)}\end{array}\right]\\&=\mathbb{D}_T(\mathcal{V}\|\mathcal{U})\end{aligned}$$

As a result, it is obviously that $\mathbb{D}_T(\mathcal{U}\|\mathcal{V})=\mathbb{D}_T(\mathcal{V}\|\mathcal{U})$.

Proof 4 *Let $\mathcal{U}$, $\mathcal{V}$ and $\mathcal{W}$ be three CFFSs over UOD Γ. In order to facilitate the proof, we first define a binary function as follows:*

$$f(x,y)=\frac{(x-y)^2}{x+y}\quad(x,y\geqslant 0)$$

Thus, $\mathbb{D}_T(\mathcal{U}\|\mathcal{V})$ can be expressed as follows:

$$\mathbb{D}_T(\mathcal{U}\|\mathcal{V})=\frac{1}{4n}\sum_{t=1}^{n}\left[\begin{array}{c}f\left(\wp_{\mathcal{U}}^3(\varsigma_t),\wp_{\mathcal{V}}^3(\varsigma_t)\right)+f\left(\gamma_{\mathcal{U}}^3(\varsigma_t),\gamma_{\mathcal{V}}^3(\varsigma_t)\right)\\+f\left(W_{\wp_{\mathcal{U}}}^3(\varsigma_t),W_{\wp_{\mathcal{V}}}^3(\varsigma_t)\right)+f\left(W_{\gamma_{\mathcal{U}}}^3(\varsigma_t),W_{\gamma_{\mathcal{V}}}^3(\varsigma_t)\right)\end{array}\right]$$

The partial derivatives of the binary function $f(x,y)$ take the following form:

$$\frac{\partial f(x,y)}{\partial x}=\frac{(x-y)(x+3y)}{(x+y)^2},$$

$$\frac{\partial f(x,y)}{\partial y}=\frac{(y-x)(3x+y)}{(x+y)^2}.$$

It follows that, if $x\leqslant y$, then $\frac{\partial f(x,y)}{\partial x}\leqslant 0$ and $\frac{\partial f(x,y)}{\partial y}\geqslant 0$. This indicates the binary function $f(x,y)$ exhibits monotonicity: it is decreasing in x and increasing in y. Similarly, if $x\geqslant y$, then $\frac{\partial f(x,y)}{\partial x}\geqslant 0$ and

$\frac{\partial f(x,y)}{\partial y} \leqslant 0$. *This indicates the binary function* $f(x,y)$ *exhibits monotonicity: it is increasing in* x *and decreasing in* y.

If $\mathcal{U} \subseteq \mathcal{V} \subseteq \mathcal{W}$, *we can obtain* $\wp_{\mathcal{U}}^3(\varsigma_t) \leqslant \wp_{\mathcal{V}}^3(\varsigma_t) \leqslant \wp_{\mathcal{W}}^3(\varsigma_t)$, $\gamma_{\mathcal{U}}^3(\varsigma_t) \geqslant \gamma_{\mathcal{V}}^3(\varsigma_t) \geqslant \gamma_{\mathcal{W}}^3(\varsigma_t)$ *and* $W_{\wp_{\mathcal{U}}}^3(\varsigma_t) \leqslant W_{\wp_{\mathcal{V}}}^3(\varsigma_t) \leqslant W_{\wp_{\mathcal{W}}}^3(\varsigma_t)$, $W_{\gamma_{\mathcal{U}}}^3(\varsigma_t) \geqslant W_{\gamma_{\mathcal{V}}}^3(\varsigma_t) \geqslant W_{\gamma_{\mathcal{V}}}^3(\varsigma_t)$.
When $x \leqslant y$, *we gain:*

$$f\left(\wp_{\mathcal{U}}^3(\varsigma_t), \wp_{\mathcal{V}}^3(\varsigma_t)\right) \leqslant f\left(\wp_{\mathcal{U}}^3(\varsigma_t), \wp_{\mathcal{W}}^3(\varsigma_t)\right), f\left(W_{\wp_{\mathcal{U}}}^3(\varsigma_t), W_{\wp_{\mathcal{V}}}^3(\varsigma_t)\right) \leqslant f\left(W_{\wp_{\mathcal{U}}}^3(\varsigma_t), W_{\wp_{\mathcal{W}}}^3(\varsigma_t)\right);$$

$$f\left(\wp_{\mathcal{V}}^3(\varsigma_t), \wp_{\mathcal{W}}^3(\varsigma_t)\right) \leqslant f\left(\wp_{\mathcal{U}}^3(\varsigma_t), \wp_{\mathcal{W}}^3(\varsigma_t)\right), f\left(W_{\wp_{\mathcal{V}}}^3(\varsigma_t), W_{\wp_{\mathcal{W}}}^3(\varsigma_t)\right) \leqslant f\left(W_{\wp_{\mathcal{U}}}^3(\varsigma_t), W_{\wp_{\mathcal{W}}}^3(\varsigma_t)\right).$$

When $x \geqslant y$, *we have:*

$$f\left(\gamma_{\mathcal{U}}^3(\varsigma_t), \gamma_{\mathcal{V}}^3(\varsigma_t)\right) \leqslant f\left(\gamma_{\mathcal{U}}^3(\varsigma_t), \gamma_{\mathcal{W}}^3(\varsigma_t)\right), f\left(W_{\gamma_{\mathcal{U}}}^3(\varsigma_t), W_{\gamma_{\mathcal{V}}}^3(\varsigma_t)\right) \leqslant f\left(W_{\gamma_{\mathcal{U}}}^3(\varsigma_t), W_{\gamma_{\mathcal{W}}}^3(\varsigma_t)\right);$$

$$f\left(\gamma_{\mathcal{V}}^3(\varsigma_t), \gamma_{\mathcal{W}}^3(\varsigma_t)\right) \leqslant f\left(\gamma_{\mathcal{U}}^3(\varsigma_t), \gamma_{\mathcal{W}}^3(\varsigma_t)\right), f\left(W_{\gamma_{\mathcal{V}}}^3(\varsigma_t), W_{\gamma_{\mathcal{W}}}^3(\varsigma_t)\right) \leqslant f\left(W_{\gamma_{\mathcal{U}}}^3(\varsigma_t), W_{\gamma_{\mathcal{W}}}^3(\varsigma_t)\right).$$

To summarize, it follows that $\mathbb{D}_T(\mathcal{U} \| \mathcal{V}) \leqslant \mathbb{D}_T(\mathcal{U} \| \mathcal{W})$ *and* $\mathbb{D}_T(\mathcal{V} \| \mathcal{W}) \leqslant \mathbb{D}_T(\mathcal{U} \| \mathcal{W})$.

4. Numerical Comparisons

In this section, four numerical examples are provided to validate the proposed divergence measure. Moreover, a detailed comparative study against existing distance measures highlights the advantages of the proposed divergence measure.

Example 1 *Consider three CFFSs, denoted as* $\mathcal{U}$, $\mathcal{V}$, *and* $\mathcal{W}$, *as follows:*

$$\mathcal{U} = \left\{\left\langle \varsigma_1, 0.5e^{2\pi i 0.3}, 0.4e^{2\pi i 0.5}\right\rangle, \left\langle \varsigma_2, 0.3e^{2\pi i 0.4}, 0.6e^{2\pi i 0.3}\right\rangle\right\},$$
$$\mathcal{V} = \left\{\left\langle \varsigma_1, 0.5e^{2\pi i 0.3}, 0.4e^{2\pi i 0.5}\right\rangle, \left\langle \varsigma_2, 0.3e^{2\pi i 0.4}, 0.6e^{2\pi i 0.3}\right\rangle\right\},$$
$$\mathcal{W} = \left\{\left\langle \varsigma_1, 0.6e^{2\pi i 0.3}, 0.4e^{2\pi i 0.7}\right\rangle, \left\langle \varsigma_2, 0.5e^{2\pi i 0.4}, 0.7e^{2\pi i 0.5}\right\rangle\right\}.$$

We can obtain the result:

$$\mathbb{D}_T(\mathcal{U} \| \mathcal{V}) = 0.0000, \mathbb{D}_T(\mathcal{V} \| \mathcal{U}) = 0.0000;$$

$$\mathbb{D}_T(\mathcal{U} \| \mathcal{W}) = 0.0351, \mathbb{D}_T(\mathcal{W} \| \mathcal{U}) = 0.0351.$$

It is confirmed by these results that the divergence measure $\mathbb{D}_T(\mathcal{U} \| \mathcal{V})$ satisfies properties 2 and 3.

Example 2 *Given three CFFSs* $\mathcal{U}$, $\mathcal{V}$ *and* $\mathcal{W}$ *expressed as follows:*

$$\mathcal{U} = \left\{\left\langle \varsigma_1, 0.2e^{2\pi i 0.1}, 0.7e^{2\pi i 0.5}\right\rangle, \left\langle \varsigma_2, 0.3e^{2\pi i 0.3}, 0.6e^{2\pi i 0.7}\right\rangle\right\},$$
$$\mathcal{V} = \left\{\left\langle \varsigma_1, 0.3e^{2\pi i 0.4}, 0.5e^{2\pi i 0.3}\right\rangle, \left\langle \varsigma_2, 0.4e^{2\pi i 0.5}, 0.5e^{2\pi i 0.4}\right\rangle\right\},$$
$$\mathcal{W} = \left\{\left\langle \varsigma_1, 0.6e^{2\pi i 0.5}, 0.4e^{2\pi i 0.2}\right\rangle, \left\langle \varsigma_2, 0.5e^{2\pi i 0.6}, 0.3e^{2\pi i 0.2}\right\rangle\right\}.$$

Then, we can get:

$$\mathbb{D}_T(\mathcal{U} \| \mathcal{V}) = 0.0662, \mathbb{D}_T(\mathcal{U} \| \mathcal{W}) = 0.1608, \mathbb{D}_T(\mathcal{V} \| \mathcal{W}) = 0.0434.$$

These results indicate that

$$\mathbb{D}_T(\mathcal{U} \| \mathcal{V}) \leqslant \mathbb{D}_T(\mathcal{U} \| \mathcal{W}), \mathbb{D}_T(\mathcal{V} \| \mathcal{W}) \leqslant \mathbb{D}_T(\mathcal{U} \| \mathcal{W}).$$

Therefore, it is clear that $\mathbb{D}_T(\mathcal{U} \| \mathcal{V})$ *fulfills the property 4.*

Example 3 *Consider two CFFSs $\mathcal{U}$ and $\mathcal{V}$ defined as follows:*

$$\mathcal{U} = \left(\mu e^{2\pi i\nu}, \nu e^{2\pi i\mu}\right), \mathcal{V} = \left(\nu e^{2\pi i\mu}, \mu e^{2\pi i\nu}\right)$$

where the parameters μ and ν are constrained to the interval $[0,1]$ and satisfy $\mu^3 + \nu^3 \leq 1$, which is presented as 1a.

The $\mathbb{D}_T\left(\mathcal{U}\,\|\mathcal{V}\right)$ between $\mathcal{U}$ and $\mathcal{V}$ is measured, with the results shown in Figure 1b. From Figure 1b, we can observe that when $\mu = \nu$, $\mathbb{D}_T\left(\mathcal{U}\,\|\mathcal{V}\right)$ attains the minimum value of 0; when $\mu = 1, \nu = 0$ or $\mu = 0, \nu = 1$, $\mathbb{D}_T\left(\mathcal{U}\,\|\mathcal{V}\right)$ reaches the maximum value of 1.

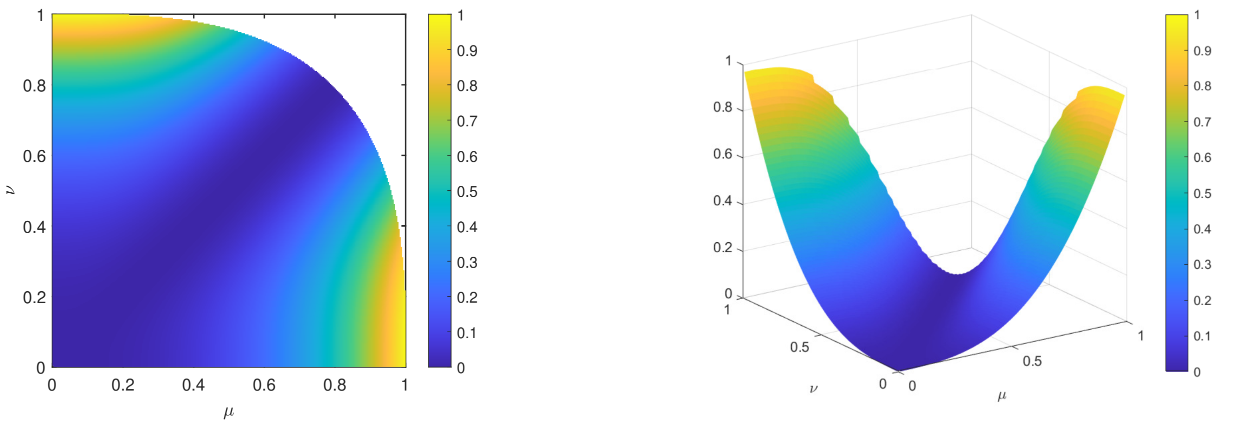

(a) $0 \leqslant \mu, \nu \leqslant 1$ **(b)** $\mu^3 + \nu^3 \leqslant 1$

Fig. 1. Results under Example 3

Thus, it is evident that $\mathbb{D}_T\left(\mathcal{U}\,\|\mathcal{V}\right)$ meets the property 1.

Example 4 *For each case i (where $i = 1, 2, 3, 4, 5, 6$), the specific numerical values of CFFSs $\mathcal{U}$ and $\mathcal{V}$ are shown in Table 1. Accordingly, the results of different distance measures with six cases are shown in Table 2.*

From the results in Table 2 and Figure 2, it follows that the existing distance measures $\mathbb{D}^1_{Ham}$, $\mathbb{D}^2_{Ham}$, $\mathbb{D}^1_{Eu}$, $\mathbb{D}^2_{Eu}$, $\mathbb{D}^1_{Hau}$ and $\mathbb{D}^2_{Hau}$ produce identical outcomes in Case 1-4, revealing their inadequacy in effectively distinguishing these cases. Likewise, the existing distance measure $\mathbb{D}_{He}$ yields the same results in Case 5 and Case 6. Despite these challenges, the proposed divergence measure for CFFSs exhibits enhanced robustness in distinguishing between various cases.

5. Post-Flood Assessment Application

In recent years, the increasing frequency of extreme weather events has led to frequent and severe flood disasters, characterized by high intensity and widespread impact. These events have caused significant disruptions to urban infrastructure, threats to population safety, and serious consequences for social and economic systems. After the flood, due to differences in topographical features, construction density, and disaster-bearing capacity, the extent of damage across different regions often exhibits significant variation. Under such uncertain, vague, and complex conditions, quickly identifying the areas that require the most urgent assistance has become a key challenge for effective disaster response and the proper allocation of recovery resources.

Table 1
Two CFFSs for six cases in Example 3

CFFS	Case 1	Case 2
$\mathcal{U}$	$\langle \varsigma, 0.7368e^{2\pi i0.7663}, 0.6694e^{2\pi i0.7047}\rangle$	$\langle \varsigma, 0.7047e^{2\pi i0.7368}, 0.6694e^{2\pi i0.5848}\rangle$
$\mathcal{V}$	$\langle \varsigma, 0.8434e^{2\pi i0.8193}, 0.5848e^{2\pi i0.5848}\rangle$	$\langle \varsigma, 0.7663e^{2\pi i0.6694}, 0.5313e^{2\pi i0.7368}\rangle$
CFFS	Case 3	Case 4
$\mathcal{U}$	$\langle \varsigma, 0.7368e^{2\pi i0.7937}, 0.6694e^{2\pi i0.5848}\rangle$	$\langle \varsigma, 0.6694e^{2\pi i0.6694}, 0.7937e^{2\pi i0.7368}\rangle$
$\mathcal{V}$	$\langle \varsigma, 0.8662e^{2\pi i0.7368}, 0.5848e^{2\pi i0.7368}\rangle$	$\langle \varsigma, 0.7368e^{2\pi i0.8193}, 0.6694e^{2\pi i0.6694}\rangle$
CCFS	Case 5	Case 6
$\mathcal{U}$	$\langle \varsigma, 0.7114e^{2\pi i0.4966}, 0.3420e^{2\pi i0.2823}\rangle$	$\langle \varsigma, 0.3969e^{2\pi i0.6300}, 0.3969e^{2\pi i0.4481}\rangle$
$\mathcal{V}$	$\langle \varsigma, 0.4481e^{2\pi i0.5872}, 0.5429e^{2\pi i0.3969}\rangle$	$\langle \varsigma, 0.4966e^{2\pi i0.3420}, 0.4966e^{2\pi i0.6300}\rangle$

Table 2
The results of various distance/divergence measures in Example 4

	Case 1	**Case 2**	**Case 3**	**Case 4**	**Case 5**	**Case 6**
$\mathbb{D}^1_{Ham}$	0.1375	0.1375	0.1625	0.1625	0.1275	0.1225
$\mathbb{D}^2_{Ham}$	0.1750	0.1750	0.2250	0.2250	0.1950	0.1650
$\mathbb{D}^1_{Eu}$	0.1436	0.1436	0.1750	0.1750	0.1543	0.1387
$\mathbb{D}^2_{Eu}$	0.1541	0.1541	0.1969	0.1969	0.1818	0.1531
$\mathbb{D}^1_{Hau}$	0.1750	0.1750	0.2250	0.2250	0.1750	0.1350
$\mathbb{D}^2_{Hau}$	0.1750	0.1750	0.2250	0.2250	0.1950	0.1650
$\mathbb{D}_{He}$	0.1185	0.1356	0.1416	0.1391	0.1936	0.1936
$\mathbb{D}_{T}$	0.0277	0.0359	0.0393	0.0380	0.0681	0.0666

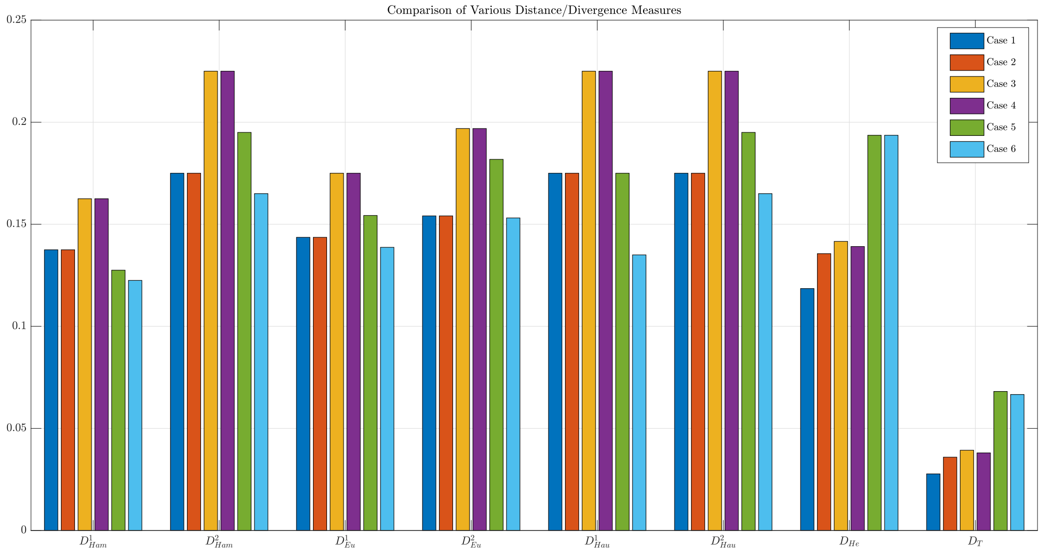

Fig. 2. Comparisons of different distance/divergence measures in six cases

To address this, we apply the novel divergence measure for CFFSs to identify and rank priority regions in post-flood assessments. Then, we define four representative flood-affected regions: traditional residential area ($\mathfrak{R}_1$), high-rise urban area ($\mathfrak{R}_2$), urban-rural fringe community ($\mathfrak{R}_3$), and urban ecological function zone ($\mathfrak{R}_4$). To comprehensively reflect the extent of damage across regions, four evaluation criteria are established for decision-making: infrastructure damage ($\mathfrak{C}_1$), population displacement ($\mathfrak{C}_2$), public service disruption ($\mathfrak{C}_3$) and economic impact ($\mathfrak{C}_4$). Based on this, the specific evaluation steps are as follows:

Step 1: Construction of the reference set

A reference set ($\mathfrak{R}$) is established to represent a severely affected region under flood conditions. Each criterion ($\mathfrak{C}_t, where\ t = 1, 2, 3, 4$) is evaluated by experts and represented by the CFFS value.

$$\mathfrak{R} = \left\{ \begin{array}{l} \langle \mathfrak{C}_1, 0.7937e^{2\pi i 0.7663}, 0.5848e^{2\pi i 0.7047} \rangle, \langle \mathfrak{C}_2, 0.7368e^{2\pi i 0.7047}, 0.6694e^{2\pi i 0.7047} \rangle \\ \langle \mathfrak{C}_3, 0.7663e^{2\pi i 0.7368}, 0.6300e^{2\pi i 0.7368} \rangle, \langle \mathfrak{C}_4, 0.6300e^{2\pi i 0.7937}, 0.7937e^{2\pi i 0.7368} \rangle \end{array} \right\}$$

Step 2: Formation of the decision matrix

Each region $\mathfrak{R}_i\ \ (i = 1, 2, 3, 4)$ is assessed separately by experts according to the four criteria $\mathfrak{C}_t$ ($t = 1, 2, 3, 4$). These evaluations are expressed using CFFSs and form a decision matrix, shown in Table 3.

Step 3: Distance calculation

The distance between each region $\mathfrak{R}_i\ \ (i = 1, 2, 3, 4)$ and the reference region $\mathfrak{R}$ is calculated using the existing distance measures and the proposed divergence measure. A smaller distance means the region is more similar to the reference, which shows it was more seriously affected by the flood and action is more urgent.

Table 3
The decision matrix is constructed for selection of the most flood-affected region

Region	$\mathfrak{C}_1$	$\mathfrak{C}_2$
$\mathfrak{R}_1$	$\langle \varsigma, 0.7937e^{2\pi i 0.7663}, 0.5848e^{2\pi i 0.7047} \rangle$	$\langle \varsigma, 0.7368e^{2\pi i 0.7047}, 0.6694e^{2\pi i 0.7047} \rangle$
$\mathfrak{R}_2$	$\langle \varsigma, 0.8193e^{2\pi i 0.6694}, 0.5848e^{2\pi i 0.7663} \rangle$	$\langle \varsigma, 0.7368e^{2\pi i 0.7663}, 0.7368e^{2\pi i 0.6694} \rangle$
$\mathfrak{R}_3$	$\langle \varsigma, 0.5848e^{2\pi i 0.7047}, 0.7047e^{2\pi i 0.7663} \rangle$	$\langle \varsigma, 0.7368e^{2\pi i 0.7937}, 0.6300^{2\pi i 0.6694} \rangle$
$\mathfrak{R}_4$	$\langle \varsigma, 0.8662e^{2\pi i 0.6300}, 0.5848e^{2\pi i 0.7937} \rangle$	$\langle \varsigma, 0.6300e^{2\pi i 0.7937}, 0.8434e^{2\pi i 0.5848} \rangle$
Region	$\mathfrak{C}_3$	$\mathfrak{C}_4$
$\mathfrak{R}_1$	$\langle \varsigma, 0.7663e^{2\pi i 0.7368}, 0.6300e^{2\pi i 0.7368} \rangle$	$\langle \varsigma, 0.6300e^{2\pi i 0.7937}, 0.7937e^{2\pi i 0.7368} \rangle$
$\mathfrak{R}_2$	$\langle \varsigma, 0.6694e^{2\pi i 0.6694}, 0.7368e^{2\pi i 0.7663} \rangle$	$\langle \varsigma, 0.7368e^{2\pi i 0.8193}, 0.5848e^{2\pi i 0.7368} \rangle$
$\mathfrak{R}_3$	$\langle \varsigma, 0.6300e^{2\pi i 0.6694}, 0.6694e^{2\pi i 0.7663} \rangle$	$\langle \varsigma, 0.7368e^{2\pi i 0.7937}, 0.5313e^{2\pi i 0.4642} \rangle$
$\mathfrak{R}_4$	$\langle \varsigma, 0.5313e^{2\pi i 0.6694}, 0.7368e^{2\pi i 0.7368} \rangle$	$\langle \varsigma, 0.7663e^{2\pi i 0.7368}, 0.5848e^{2\pi i 0.7663} \rangle$

Step 4: Priority Ranking of Regions

To clearly identify the most affected region, the computed values are sorted in ascending order, namely $\mathfrak{R}_1 < \mathfrak{R}_2 < \mathfrak{R}_4 < \mathfrak{R}_3$. As shown in Table 4, all distance results indicate that $\mathfrak{R}_1$, traditional residential area, has the closest value to the reference set. This suggests that the traditional residential area ($\mathfrak{R}_1$) experiences the most severe flood impact and should receive priority in recovery efforts. The result provides practical guidance for government departments and emergency responders on organizing recovery efforts following the flood.

Step 5: Evaluation of DoC

Although the results from different distance measures are consistent, their ability to accurately identify the most affected region differs. Thus, further analysis is needed. For example, $\mathbb{D}^1_{Ham}$ and $\mathbb{D}^1_{Hau}$ produce identical results for both $\mathfrak{R}_2$ and $\mathfrak{R}_4$. Therefore, a new performance metric, known as the Degree of Confidence (DoC), is introduced by Hatzimichailidis *et al.* [38]. This factor assesses the confidence level of distance/divergence measures in accurately identifying a region as belonging to class t and is defined by the following formula Eq. (15). The results are represented in Table 4.

$$DoC = \sum_{i=1, i \neq t}^{n} \left| D\left(\mathfrak{R}_t, \mathfrak{R}\right) - D\left(\mathfrak{R}_i, \mathfrak{R}\right) \right| \tag{15}$$

Based on the results in Table 4 and Figure 3, $\mathbb{D}_T$ shows higher DoC values. This indicates that the proposed divergence measure is the most confident in identifying $\mathfrak{R}_1$ as the area most severely affected by the flood. This analysis can help decision-makers determine the most reliable divergence measure for this situation and inform their next steps.

Table 4
The results of distance/divergence measures and DoC

	$(\mathfrak{R}_1, \mathfrak{R})$	$(\mathfrak{R}_2, \mathfrak{R})$	$(\mathfrak{R}_3, \mathfrak{R})$	$(\mathfrak{R}_4, \mathfrak{R})$	Ranking	Result	DoC
$\mathbb{D}^1_{Ham}$	0.0844	0.1344	0.2094	0.1344	$\mathfrak{R}_1 < \mathfrak{R}_2 = \mathfrak{R}_4 < \mathfrak{R}_3$	$\mathfrak{R}_1$	1.3331
$\mathbb{D}^2_{Ham}$	0.1125	0.1750	0.2875	0.1875	$\mathfrak{R}_1 < \mathfrak{R}_2 < \mathfrak{R}_4 < \mathfrak{R}_3$	$\mathfrak{R}_1$	1.4098
$\mathbb{D}^1_{Eu}$	0.0927	0.1442	0.2274	0.1452	$\mathfrak{R}_1 < \mathfrak{R}_2 < \mathfrak{R}_4 < \mathfrak{R}_3$	$\mathfrak{R}_1$	1.3293
$\mathbb{D}^2_{Eu}$	0.1173	0.1571	0.2568	0.1732	$\mathfrak{R}_1 < \mathfrak{R}_2 < \mathfrak{R}_4 < \mathfrak{R}_3$	$\mathfrak{R}_1$	1.2340
$\mathbb{D}^1_{Hau}$	0.0938	0.1750	0.2750	0.1750	$\mathfrak{R}_1 < \mathfrak{R}_2 = \mathfrak{R}_4 < \mathfrak{R}_3$	$\mathfrak{R}_1$	1.5125
$\mathbb{D}^2_{Hau}$	0.1125	0.1750	0.2875	0.1875	$\mathfrak{R}_1 < \mathfrak{R}_2 < \mathfrak{R}_4 < \mathfrak{R}_3$	$\mathfrak{R}_1$	1.4098
$\mathbb{D}_{He}$	0.0770	0.1240	0.2102	0.1319	$\mathfrak{R}_1 < \mathfrak{R}_2 < \mathfrak{R}_4 < \mathfrak{R}_3$	$\mathfrak{R}_1$	1.5006
$\mathbb{D}_T$	0.0118	0.0302	0.0820	0.0338	$\mathfrak{R}_1 < \mathfrak{R}_2 < \mathfrak{R}_4 < \mathfrak{R}_3$	$\mathfrak{R}_1$	2.7148

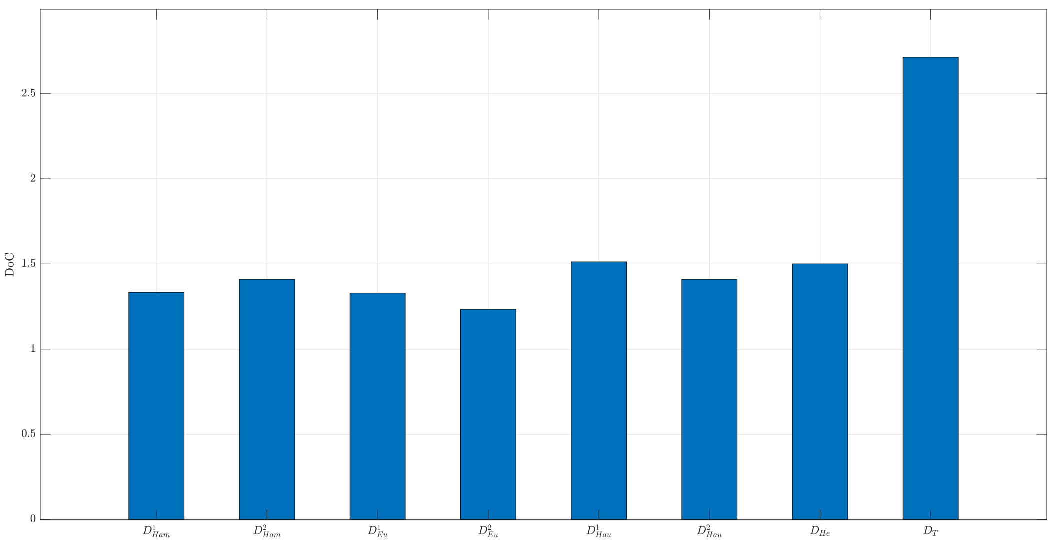

Fig. 3. The values of DoC for the distance/divergence measures

6. Conclusions

This paper introduces a new divergence measure based on CFFSs to address the limitations of existing measures. We thoroughly analyze the mathematical properties of the proposed divergence measure, proving their non-negativity, and symmetry, and other key characteristics. These properties ensure that our measure is not only theoretically sound but also practical for use in real-world decision-making problems. Several numerical comparisons are conducted to assess the performance of the proposed measure against existing distance measures for complex fuzzy setting. The results demonstrate that the new measure outperforms previous measures in terms of flexibility and accuracy. Furthermore, the proposed measure is validated through an application involving post-flood region prioritization, where it effectively captures the critical factors for decision-making, showcasing its practical utility. While this study represents a significant advancement in the theory and application of CFFSs, there are still several avenues for future research. For instance, further exploration could focus on developing additional aggregation operators and optimization algorithms that leverage the divergence measure for multi-criteria decision analysis. Additionally, extending the application of CFFSs to other areas, such as medical diagnosis, environmental monitoring, and artificial intelligence, could further demonstrate the versatility and effectiveness of the proposed measure.

Acknowledgement

This research was not funded by any grant.

Conflicts of Interest

The authors declare no conflicts of interest.

References

[1] Sadana, U., Chenreddy, A., Delage, E., Forel, A., Frejinger, E., & Vidal, T. (2025). A survey of contextual optimization methods for decision-making under uncertainty. *European Journal of Operational Research*, *320(2)*, 271–289. https://doi.org/10.1016/j.ejor.2024.03.020

[2] Zhang, C., Xia, P., & Zhang, X. (2024). Multi-attribute decision-making method of pumped storage capacity planning considering wind power uncertainty. *Journal of Cleaner Production*, *449*, 141655. https://doi.org/10.1016/j.jclepro.2024.141655

[3] Hedayatipour, M., Etemadi, S., Hekmat, S. N., & Moosavi, A. (2024). Challenges of using evidence in managerial decision-making of the primary health care system. *BMC Health Services Research*, *24(1)*, 38. https://doi.org/10.1186/s12913-023-10409-7

[4] Liu, Z., & Letchmunan, S. (2024). Enhanced fuzzy clustering for incomplete instance with evidence combination. *ACM Transactions on Knowledge Discovery from Data*, *18(3)*, 1–20. https://doi.org/10.1145/3638061

[5] Asif, M., Ishtiaq, U., & Argyros, I. K. (2025). Hamacher aggregation operators for pythagorean fuzzy set and its application in multi-attribute decision-making problem. *Spectrum of Operational Research*, *2(1)*, 27–40. https://doi.org/10.31181/sor2120258

[6] Liu, Z., Zhu, S., Senapati, T., Deveci, M., Pamucar, D., & Yager, R. R. (2025). New distance measures of complex fermatean fuzzy sets with applications in decision making and clustering problems. *Information Sciences*, *686*, 121310. https://doi.org/10.1016/j.ins.2024.121310

[7] Yousafzai, F., Zia, M. D., Khalaf, M. M., Ismail, R., et al. (2024). Linear diophantine fuzzy sets over complex fuzzy information with applications in information theory. *Ain Shams Engineering Journal*, *15(1)*, 102327. https://doi.org/10.1016/j.asej.2023.102327

[8] Wang, C., Song, Z., & Fan, H. (2024). Novel evidence theory-based reliability analysis of functionally graded plate considering thermal stress behavior. *Aerospace Science and Technology*, *146*, 108936. https://doi.org/10.1016/j.ast.2024.108936

[9] Zadeh, L. A. (1965). Fuzzy sets. *Information and Control*, *8(3)*, 338–353. https://doi.org/10.1016/S0019-9958(65)90241-X

[10] Atanassov, K. T. (1986). Intuitionistic fuzzy sets. *Fuzzy Sets and Systems*, *20*, 87–96. https://doi.org/10.1016/s0165-0114(86)80034-3

[11] Huang, W., Zhang, F., Wang, S., & Kong, F. (2024). A novel knowledge-based similarity measure on intuitionistic fuzzy sets and its applications in pattern recognition. *Expert Systems with Applications*, *249*, 123835. https://doi.org/10.1016/j.eswa.2024.123835

[12] Alreshidi, N. A., Shah, Z., & Khan, M. J. (2024). Similarity and entropy measures for circular intuitionistic fuzzy sets. *Engineering Applications of Artificial Intelligence*, *131*, 107786. https://doi.org/10.1016/j.engappai.2023.107786

[13] Yager, R. R. (2014). Pythagorean membership grades in multicriteria decision making. *IEEE Transactions on Fuzzy Systems*, *22(4)*, 958–965. https://doi.org/10.1109/TFUZZ.2013.2278989

[14] Li, R., Ejegwa, P. A., Li, K., Agaji, I., Feng, Y., & Onyeke, I. C. (2024). A new similarity function for pythagorean fuzzy sets with application in football analysis. *AIMS Mathematics*, *9(2)*, 4990–5014. https://doi.org/10.3934/math.2024242

[15] Liu, Z. (2024a). Hellinger distance measures on pythagorean fuzzy environment via their applications. *International Journal of Knowledge-Based and Intelligent Engineering Systems*, *28(2)*, 211–229. https://doi.org/10.3233/kes-230150

[16] Akram, M., Luqman, A., Alcantud, J. C. R., et al. (2022). An integrated electre-i approach for risk evaluation with hesitant pythagorean fuzzy information. *Expert Systems with Applications*, *200*, 117002. https://doi.org/10.1016/j.eswa.2022.116945

[17] Senapati, T., & Yager, R. R. (2020). Fermatean fuzzy sets. *Journal of Ambient Intelligence and Humanized Computing*, *11*, 663–674. https://doi.org/10.1007/s12652-019-01377-0

[18] Büyüközkan, G., Uztürk, D., & Ilıçak, Ö. (2024). Fermatean fuzzy sets and its extensions: A systematic literature review. *Artificial Intelligence Review*, *57(6)*, 138. https://doi.org/10.1007/s10462-024-10761-y

[19] Yu, J., Ding, H., Yu, Y., Wu, S., Zeng, Q., & Xu, Y. (2024). Risk assessment of liquefied natural gas storage tank leakage using failure mode and effects analysis with fermatean fuzzy sets and cocoso method. *Applied Soft Computing*, *154*, 111334. https://doi.org/10.1016/j.asoc.2024.111334

[20] Ramot, D., Milo, R., Friedman, M., & Kandel, A. (2002). Complex fuzzy sets. *IEEE Transactions on Fuzzy Systems*, *10(2)*, 171–186. https://doi.org/10.1109/91.995119

[21] Alkouri, M. J. S., & Salleh, A. R. (2012). Complex intuitionistic fuzzy sets. *AIP Conference Proceedings*, *1482(1)*, 464–470. https://doi.org/10.1063/1.4757515

[22] Wang, P., Zhu, B., Yu, Y., Ali, Z., & Almohsen, B. (2023). Complex intuitionistic fuzzy dombi prioritized aggregation operators and their application for resilient green supplier selection. *Facta Universitatis, Series: Mechanical Engineering*, *21(3)*, 339–357. https://doi.org/10.22190/fume230805029w

[23] Liu, P., & Ali, Z. (2024). Hamacher interaction aggregation operators for complex intuitionistic fuzzy sets and their applications in green supply chain management. *Complex & Intelligent Systems*, *10(3)*, 3853–3871. https://doi.org/10.1007/s40747-023-01329-4

[24] Mahmood, T., Ullah, K., Ali, Z., & Siddique, I. (2020). Complex pythagorean fuzzy sets and their applications in decision-making. *Complex & Intelligent Systems*, *6*, 111–122. https://doi.org/10.1007/s40747-019-0103-6

[25] Labassi, F., Rehman, U. U., Alsuraiheed, T., Mahmood, T., & Khan, M. A. (2024). A novel approach toward complex pythagorean fuzzy sets and their applications in visualization technology. *IEEE Access*, *12*, 65838–65855. https://doi.org/10.1109/access.2024.3393138

[26] Khan, M. S. (2025). Intelligent image segmentation via complex pythagorean fuzzy sets and level-set optimization. *International Journal of Knowledge and Innovation Studies*, *3(1)*, 50–59. https://doi.org/10.56578/ijkis030105

[27] Rahman, K., Garg, H., Ali, R., Alfalqi, S. H., & Lamoudan, T. (2023). Algorithms for decision-making process using complex pythagorean fuzzy set and its application to hospital siting for

covid-19 patients. *Engineering Applications of Artificial Intelligence*, *126*, 107153. https://doi.org/10.1016/j.engappai.2023.107153

[28] Akram, M., Amjad, U., Alcantud, J. C. R., & Santos-García, G. (2023). Complex fermatean fuzzy n-soft sets: A new hybrid model with applications. *Journal of Ambient Intelligence and Humanized Computing*, *14(7)*, 8765–8798. https://doi.org/10.1007/s12652-021-03629-4

[29] Ali, R., Rahman, K., & Muhammad, J. (2024). Complex fermatean fuzzy models and their algebraic aggregation operators in decision-making: A case study on covid-19 vaccine selection. *J. Oper. Strat. Anal.*, *2*, 119–135. https://doi.org/10.56578/josa020205

[30] Zaman, M., Ghani, F., Khan, A., Abdullah, S., & Khan, F. (2023). Complex fermatean fuzzy extended topsis method and its applications in decision making. *Heliyon*, *9*(9), e19170. https://doi.org/10.1016/j.heliyon.2023.e19170

[31] Garg, H., Dutta, D., Dutta, P., & Gohain, B. (2024). An extended group decision-making algorithm with intuitionistic fuzzy set information distance measures and their applications. *Computers & Industrial Engineering*, *197*, 110537. https://doi.org/10.1016/j.cie.2024.110537

[32] Liu, Z. (2024b). A distance measure of fermatean fuzzy sets based on triangular divergence and its application in medical diagnosis. *Journal of Operations Intelligence*, *2*(1), 167–178. https://doi.org/10.31181/jopi21202415

[33] Wu, X., Liu, Q., Liu, L., Yang, M.-S., & Zhang, X. (2025). New jensen–shannon divergence measures for intuitionistic fuzzy sets with the construction of a parametric intuitionistic fuzzy topsis. *Complex & Intelligent Systems*, *11*(2), 1–15. https://doi.org/10.1007/s40747-024-01761-0

[34] Gohain, B., Chutia, R., & Dutta, P. (2022). Distance measure on intuitionistic fuzzy sets and its application in decision-making, pattern recognition, and clustering problems. *International Journal of Intelligent Systems*, *37*(3), 2458–2501. https://doi.org/10.1002/int.22780

[35] Ganie, A. H., Gheith, N. E. M., Al-Qudah, Y., Ganie, A. H., Sharma, S. K., Aqlan, A. M., & Khalaf, M. M. (2024). An innovative fermatean fuzzy distance metric with its application in classification and bidirectional approximate reasoning. *IEEE Access*, *12*, 4780–4791. https://doi.org/10.1109/ACCESS.2023.3348780

[36] Rani, D., & Garg, H. (2017). Distance measures between the complex intuitionistic fuzzy sets and their applications to the decision-making process. *International Journal for Uncertainty Quantification*, *7*(5), 423–439. https://doi.org/10.1615/Int.J.UncertaintyQuantification.2017020356

[37] Ullah, K., Mahmood, T., Ali, Z., & Jan, N. (2020). On some distance measures of complex pythagorean fuzzy sets and their applications in pattern recognition. *Complex & Intelligent Systems*, *6*(1), 15–27. https://doi.org/10.1007/s40747-019-0103-6

[38] Hatzimichailidis, A. G., Papakostas, G. A., & Kaburlasos, V. G. (2012). A novel distance measure of intuitionistic fuzzy sets and its application to pattern recognition problems. *International Journal of Intelligent Systems*, *27(4)*, 396–409. https://doi.org/10.1002/int.21529